SULFIDE–SULFATE CHIMNEYS ON THE EAST PACIFIC RISE, 11° AND 13°N LATITUDES. PART I: MINERALOGY AND PARAGENESIS

URSULA M. GRAHAM, GREGG J. BLUTH AND HIROSHI OHMOTO

Department of Geosciences, The Pennsylvania State University, University Park, Pennsylvania 16802, U.S.A.

ABSTRACT

Hydrothermal fluids up to ~350°C emerge from vent sites at 11° and 13°N latitudes, East Pacific Rise. Variations in the morphology, zoning and mineralogy of 27 chimneys from 11 vent sites can be represented by three active and one extinct-clogged chimney. Microscopic observation of 127 polished sections of these four chimneys has revealed four types each of marcasite, pyrite and wurtzite, and two types of sphalerite, which are distinct in their crystal habits. The consistency in the paragenetic sequence and in the spatial distribution with respect to the exterior chimney wall of these Fe and Zn sulfides, as well as anhydrite, chalcopyrite and bornite in these four chimneys suggests that all chimneys in the 11 vent sites represent similar hydrothermal processes. The variation among the chimneys reflects simply the difference in the maturity (longevity of venting) and preservation of a complete (ideal) chimney, which is comprised of 8 mineralogical zones. Formation of zone-1 minerals (anhydrite with minor subhedral pyrite, and anhedral marcasite and wurtzite) takes place during mixing of hydrothermal fluids and cold seawater when the rate of mineral precipitation exceeds mineral dissolution by cold seawater. During outward growth of a chimney, zone-1 minerals are continuously dissolved by later hydrothermal fluids, and also metasomatically transformed successively to zone 2 (mostly large colloform marcasite and wurtzite), zone 3 (mostly cubes of pyrite and colloform sphalerite), zone 4 (mostly bornite), and zone 5 (mostly chalcopyrite); some new minerals (*e.g.*, cubes of pyrite, sphalerite, chalcopyrite) also precipitate directly from the hydrothermal fluids within the pore space created by the dissolution of zone-1 minerals. With continued venting, channel openings enlarge, and each sulfide zone tends to become wider and monomineralic; the width of the anhydrite-rich zone 1, however, becomes larger during early venting and then decreases with time. Clogging of a chimney occurs during the waning stage of hydrothermal activity, by precipitation of zone-7 and -8 minerals (wurtzite, marcasite and pyrite) along the inner chalcopyrite wall of zone 5, and recrystallization in time to form zone 6 (mostly pyrite and sphalerite). With decreasing hydrothermal activity, the chimney walls begin to dissolve from the outside by reaction with cold seawater. The observed paragenesis suggests that the rates of cooling and oxidation, as well as the metal-sulfur chemistry of hydrothermal fluids, are important parameters that control the chimney mineralogy. Quenching of H_2S-rich fluids, caused by rapid mixing with cold seawater, may result in precipitation of pyrrhotite and wurtzite, while anhydrite precipitates by incorporating SO_4^{2-} of local seawater. Anhydrite layers formed by such a process may play important roles both physically and chemically in the development of sulfide mineralogy within the chimney walls by creating environments that promote not only oxidation of hydrothermal H_2S to generate polysulfide

species for FeS_2, but also recrystallization and replacement of earlier minerals in warmer conditions.

Keywords: chimneys, hydrothermal, sulfides, sulfates, mineralogy, zoning, paragenesis, East Pacific Rise.

SOMMAIRE

Des fluides hydrothermaux atteignant une température d'environ 350°C sont émis des évents aux latitudes 11° et 13°N, le long de la ride Est-Pacifique. Les variations en morphologie, zonation et minéralogie de 27 cheminées provenant de 11 sites sont bien représentées par trois cheminées actives et une éteinte qui est engorgée de dépôts. Un examen par microscopie de 127 sections prélevées de ces quatre cheminées révèle la présence de quatre générations de marcasite, pyrite et wurtzite, et deux de sphalérite, distinguées par leur habitus. La concordance dans la séquence paragénétique de ces sulfures de Fe et de Zn, de l'anhydrite, de la chalcopyrite et de la bornite, aussi bien que dans leur distribution par rapport à la paroi externe, fait penser que toute cheminée des 11 sites d'évents résulte de processus hydrothermaux semblables, et que les variations entre les cheminées s'expliquent simplement par les différences en maturité (durée de l'émission) et en degré de préservation d'une cheminée complète idéale, qui comprend huit zones minéralogiques. Les minéraux de la zone 1 (anhydrite, pyrite sub-idiomorphe accessoire, avec marcasite non-idiomorphe et wurtzite) se sont formés lors du mélange entre le fluide hydrothermal et l'eau de mer froide, lorsque le taux de précipitation est supérieur au taux de dissolution des minéraux dans l'eau de mer ambiante. Pendant la croissance excentrique d'une cheminée, les minéraux de la zone 1 sont continuellement redissous par les fluides hydrothermaux plus jeunes, ainsi que transformés par métasomatoses successives en assemblages des zones 2 (principalement de la marcasite colloforme à grains grossiers et de la wurtzite), 3 (principalement des cubes de pyrite et de la sphalérite colloforme), 4 (principalement de la bornite), et 5 (principalement de la chalcopyrite). Certains minéraux (par exemple, cubes de pyrite, sphalérite et chalcopyrite) sont aussi directement précipités des fluides hydrothermaux dans les pores créés par la dissolution des minéraux de la zone 1. À mesure que l'émission progresse, les orifices s'élargissent, et chaque zone de sulfures tend à devenir plus large et monominéralique, excepté la zone 1, qui s'élargit pendant les stades précoces pour ensuite diminuer au cours de l'évolution d'un évent. L'engorgement d'une cheminée caractérise les stades terminaux de l'activité hydrothermale, lors de la précipitation des minéraux des zones 7 et 8 (wurtzite, marcasite et pyrite) le long de la paroi interne de chalcopyrite de la zone 5, et de leur recristallisation éventuelle pour former la zone 6 (principalement de la pyrite et de la sphalérite). Au cours de la diminution de l'activité, les parois d'une cheminée sont progressivement dissous par

réaction avec l'eau de mer froide. La séquence paragénétique observée indique que les taux de refroidissement et d'oxydation, aussi bien que les relations chimiques entre métaux et soufre dans les fluides hydrothermaux, exercent un contrôle important sur la composition minéralogique d'une cheminée. Un refroidissement brutal de fluides riches en H_2S par mélange rapide avec l'eau de mer pourrait causer la précipitation de pyrrhotite et de wurtzite, tandis que l'anhydrite serait précipitée par incorporation du SO_4^{2-} provenant de l'eau de mer ambiante. Les niveaux d'anhydrite ainsi formés pourrait jouer des rôles physique et chimique importants dans le développement de la minéralogie des sulfures à l'intérieur des parois d'une cheminée en créant des milieux qui, non seulement provoquent l'oxydation du H_2S hydrothermal pour permettre la formation d'espèces polysulfurées aux dépens du FeS_2, mais aussi facilitent la recristallisation et le remplacement des minéraux précoces dans les milieux plus chauds.

(Traduit par la Rédaction)

Mots-clés: cheminées, hydrothermal, sulfures, sulfates, minéralogie, zonation, paragenèse, ride Est-Pacifique.

INTRODUCTION

Within the past decade, hydrothermal systems actively depositing sulfides of Cu, Fe, and Zn have been examined at numerous locations along oceanic spreading ridges. The strongest manifestation of hydrothermal activity occurs within axial grabens (Hékinian *et al.* 1983, Ballard *et al.* 1984). The hydrothermal vents discharge metal- and H_2S-rich, acidic, high-temperature (up to ~350°C) fluids into cold seawater; sulfide and sulfate minerals precipitate from the mixtures of hydrothermal fluids and seawater.

Precipitates from high-temperature vents seem to represent the modern equivalents of ancient massive sulfide deposits, and as such, provide a unique opportunity to document ore-forming processes. Similarities between ancient and modern massive Fe–Cu–Zn sulfide deposits include: (1) deposition on the ocean floor at depths >2000 m; (2) formation of the main sulfide phases by reactions of hot (~150–350°C) fluids with cold seawater; (3) sulfides of Fe, Cu, and Zn as the dominant metal-bearing phases (Styrt *et al.* 1981, Ohmoto & Skinner 1983, Ohmoto 1988). The advantage of studying these modern systems is that the processes and products of active mineralization can be observed, and the deposits can be sampled in their unaltered state without the complexities introduced by metamorphism and deformation.

Sulfide deposits along the East Pacific Rise (EPR) near 11°, 13°, and 21°N, and on the southern Juan de Fuca Ridge have similar geological settings (Hékinian *et al.* 1980 1983, Hékinian & Fouquet 1985, Ballard *et al.* 1984, Koski *et al.* 1983, McConachy *et al.* 1986, Normark *et al.* 1986). The mineralogy and chemistry of samples from active and extinct hot-spring sites along 21°N EPR have been studied by Haymon & Kastner (1981), Oudin (1983), Goldfarb *et al.* (1983), and Haymon (1983). Larger, structurally more complex sulfide deposits than those from 21°N have been found on the Endeavor and Middle Valley Segments of the Juan de Fuca Ridge, and are described respectively by Tivey & Delaney (1986) and Tunnicliffe *et al.* (1986). The chemical evolution of ocean-ridge hot springs is described by Bowers *et al.* (1985), and a laboratory and theoretical study of the growth of black-smoker chimneys is given by Turner & Campbell (1987).

Chimney samples from the vent sites studied by previous workers are similar in many respects. For example, the chimneys consist dominantly of chalcopyrite, pyrite, wurtzite (sphalerite), and anhydrite, although their proportions vary greatly among the chimneys. There are regularities in mineralogical zonation, with a nearly monomineralic chalcopyrite layer at the interior walls of the chimneys, and an increase towards the exteriors in the abundance of disseminated Fe and Zn sulfides associated with anhydrite. Replacement and overgrowth textures among sulfides are also common to all chimney structures.

Previous investigators recognized that minerals in the chimneys were formed by two concurrent processes: direct precipitation from the mixed solutions of hot fluid and cold seawater, and replacement or recrystallization of the earlier minerals within the chimney wall (*e.g.*, Goldfarb *et al.* 1983, Hékinian *et al.* 1983, Tivey & Delaney 1986). Initial chimney growth starts with the rapid precipitation of anhydrite and minor sulfides to establish a permeable chimney wall (Goldfarb *et al.* 1983, Haymon 1983). The wall functions as a partial barrier between hydrothermal fluid and seawater, restricting their mixing. At subsequent higher temperatures within the chimney, mineral precipitation and replacement create the observed sulfide–sulfate zoning sequences. Variations in the relative abundance of sulfide to sulfate can be related to the growth stages or relative maturity of the vent structures (Goldfarb *et al.* 1983). These authors suggested that differences in the Cu/Zn ratio in chimneys from 21°N were controlled by the thermal history of the hydrothermal fluids: Zn-rich chimneys formed from fluids of T < ~300°C, and Cu-rich chimneys formed from fluids of T > ~300°C.

Nevertheless, many questions about chimney growth and sulfide mineralogy remained. Problems requiring further study involved: i) the temporal and spatial relationships between marcasite and pyrite, and between wurtzite and sphalerite; ii) the dominance of pyrrhotite in the smoke, but of marcasite and pyrite in the chimney walls; iii) the restriction of abundant chalcopyrite to inner chimney walls and its near-absence from the smoke; and iv) the causes of both regularities and variability in the

mineral zoning. The major objectives of this study were, therefore, to put constraints on the above problems by investigating in detail the mineralogy and paragenesis, both of active and extinct chimneys, from 11° and 13°N. This study also serves as the framework for a sulfur isotope study reported in the accompanying paper by Bluth & Ohmoto (1988).

SAMPLES

The chimney samples used in this study were collected by L.K. Reilly of The Pennsylvania State University, J.M. Edmond of The Massachusetts Institute of Technology, and other members of the 1984 ALVIN expedition at 13°N (dives 1366 through 1375), and 11°N (dives 1377 through 1380) of the EPR. Their geologic settings are described by Ballard *et al.* (1984) and McConachy *et al.* (1986).

A total of 27 chimney samples from 11 vent sites was examined macroscopically for the preservation of vent structures, porosity, mineral abundances, zonation, thickness of individual mineral layers, and crystallinity of minerals. The general appearance of the chimneys varied, particularly the thickness and relative positions of mineral layers; measured discharge temperatures also differed at the active vents. Four chimneys, representative of the range of vent structures at 11° and 13°N, were selected for detailed investigation (locations in Fig. 1). Three chimneys (A, B, C) were active when sampled; the fourth (D) was extinct.

Chimney A (anhydrite-rich)

This chimney was sampled from vent site #7 (12° 49′N) where hydrothermal fluids were emitting at 380°C, although this temperature has been questioned (Bowers *et al.* 1988). The recovered part of the vent structure is 64 cm long, averages 20 cm in diameter, and branches upward into two individual conduits (Fig. 2a). The outer parts of the chimney walls are composed largely of anhydrite and disseminated (~5% in volume) sulfides (pyrite + marcasite + wurtzite + chalcopyrite; Fig. 3a). A 10–50 μm-wide bornite-rich layer and a 1–5 mm-thick chalcopyrite-rich layer line the inner wall.

Chimney B (Zn- and Fe-rich)

Chimney B, collected from vent site #10 (10°58′N), consists of four individual conduits (Fig. 2b). Only one conduit was active when sampled; the fluids were discharging at 347°C. This conduit was selected for microscopic study. It is 30 cm long, with chimney walls averaging 6 cm in thickness. The active conduit is characterized by a thin (~1 mm) exterior layer of anhydrite, a thick (~4 cm) transition zone of marcasite + wurtzite + pyrite, and an inner lining (~2 cm) of nearly monomineralic chalcopyrite
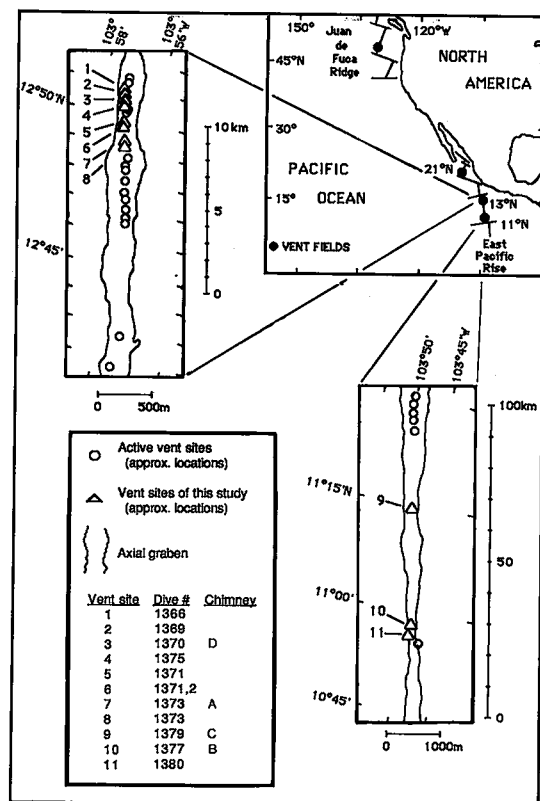
FIG. 1. Locations of chimney samples collected from 11° and 13° N latitudes, EPR, during the ALVIN dives in May–June, 1984. After Ballard *et al.* (1984), L.K. Reilly (pers. comm. 1985), and A.C. Campbell (pers. comm. 1986).

(Fig. 3b). A bornite-rich zone (~0.5 cm) occurs immediately externally to the chalcopyrite layer.

Chimney C (Cu-rich)

Chimney C was collected from vent site #9 (11°14′N). The temperature of the hydrothermal fluids was not measured. The chimney consists of a single 69-cm-long conduit, and has an average wall thickness of 15 cm (Fig. 2c); five auxiliary conduits are also present. The outer two-thirds of the chimney consists of massive sulfides of Zn and Fe, whereas the interior one-third (~5 cm) is rich in chalcopyrite (Fig. 3c). Anhydrite is not visible macroscopically at the chimney exterior, but was recognized microscopically and by X-ray diffraction analyses.

Chimney D (inversely zoned)

This extinct chimney, from vent site #3 (12°51′N), is 25 cm long with walls ~3 cm thick; the top is
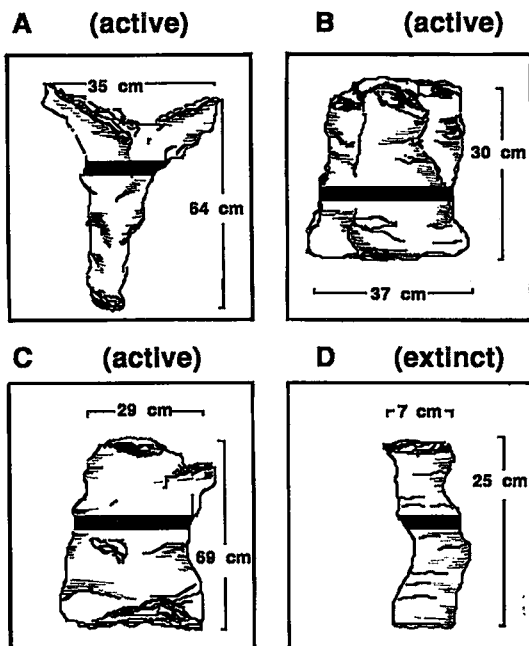
FIG. 2. Sketches of the four chimneys (A–D) investigated in detail.

clogged with sulfides (Fig. 2d). The most striking feature of this chimney is the reverse mineralogical zoning compared to active chimneys A, B, and C. The exterior wall is a chalcopyrite-rich layer ~ 1cm thick; the inside is filled by marcasite, pyrite, wurtzite and sphalerite (Fig. 3d). Anhydrite is not present.

The preservation of anhydrite in the chimney walls and the spatial relationship among various sulfide layers are the criteria on which we base our estimate of the relative ages of the chimneys. In our model, Chimney A is the youngest vent type, followed successively by B, C, and D. Chimneys of type A and B are most common among the 27 samples. Type D is represented by only one sample.

TEXTURES, PARAGENESIS AND COMPOSITIONS
OF CHIMNEY MINERALS

Cross-sectional slices of the base, center and top of each chimney structure were prepared. A total of 127 polished and doubly polished thin sections was examined, representing 19 traverses from the outside to the inside walls of chimneys A through D. Reflected- and transmitted-light microscopy, X-ray diffraction, and electron-microprobe analyses were used for mineral indentification and textural interpretation. Microprobe analyses were carried out on wurtzite, Cu–Fe sulfides, pyrite and marcasite.

In general, pyrite and marcasite are the most abundant sulfides in the outer parts of the active chimneys, followed by wurtzite. The Cu–Fe sulfides are primarily chalcopyrite, isocubanite, and bornite. Along the conduit (and the exterior wall of Chimney D), chalcopyrite is the dominant sulfide (up to 90 vol.%). Isocubanite represents less than 10% of total Cu–Fe sulfides. Bornite and covellite can be the dominant phases in particular zones, but account for less than a few percent of total Cu-bearing sulfides in a chimney. Traces of digenite and chalcocite are present. Sphalerite constitutes between 0–80% of total Zn sulfides within the different zones, and generally occurs internally to the wurtzite, except in the extinct chimney. Pyrrhotite (<1%) was observed only in the innermost layer of Chimney C. The pyrrhotite occurs as inclusions in chalcopyrite and in pyrite cubes as prismatic and strongly fractured crystals. Non-sulfide phases include anhydrite, minor barite (<5% of total sulfate) and amorphous silica (<5% of the total mineral assemblage); they occur only at the exterior walls of chimneys A and B.

Anhydrite

Anhydrite may form up to 70 vol. % of the wall in Chimney A. Anhydrite crystals (100–600 μm) are predominantly perpendicular to channelways; banded structures and oval clusters up to 1 cm in diameter are also present. Anhydrite forms a broad outer wall in Chimney A, a thin rim in Chimney B, and a minor dissemination in the outermost zone of Chimney C. Anhydrite is not observed in extinct Chimney D. The anhydrite zone in chimneys B and C could have originally been as thick as that in Chimney A, but appear to have eroded, probably due to the continuous reactions with hydrothermal fluids and with seawater; corroded remnants and replacement textures (pseudomorphs) of anhydrite by marcasite and wurtzite are common in the outermost zone of chimneys B and C.

Iron sulfides

Four types of pyrite and four types of marcasite have been distinguished based on differences in their grain size, crystal habit, crystallinity, porosity and inclusions of other sulfides. In general, pyrite is the most abundant Fe sulfide in all samples; it accounts for about 40 vol.% of Chimney B.

Important characteristics of the four types of pyrite are summarized in Table 1. Pyrite-1 consists of euhedral cubic and pyritohedral crystals, 5–50 μm across, but usually <10 μm. It occurs within the anhydrite walls of Chimney A (Fig. 4a) and is a minor constituent of the interior walls of active chimneys, but is absent from extinct Chimney D.

Pyrite-2, the most abundant type in the active chimneys, occurs as coarse-grained (100–500 μm), subhedral to euhedral crystals and their clusters. Some of the clusters form semilinear to curved bands
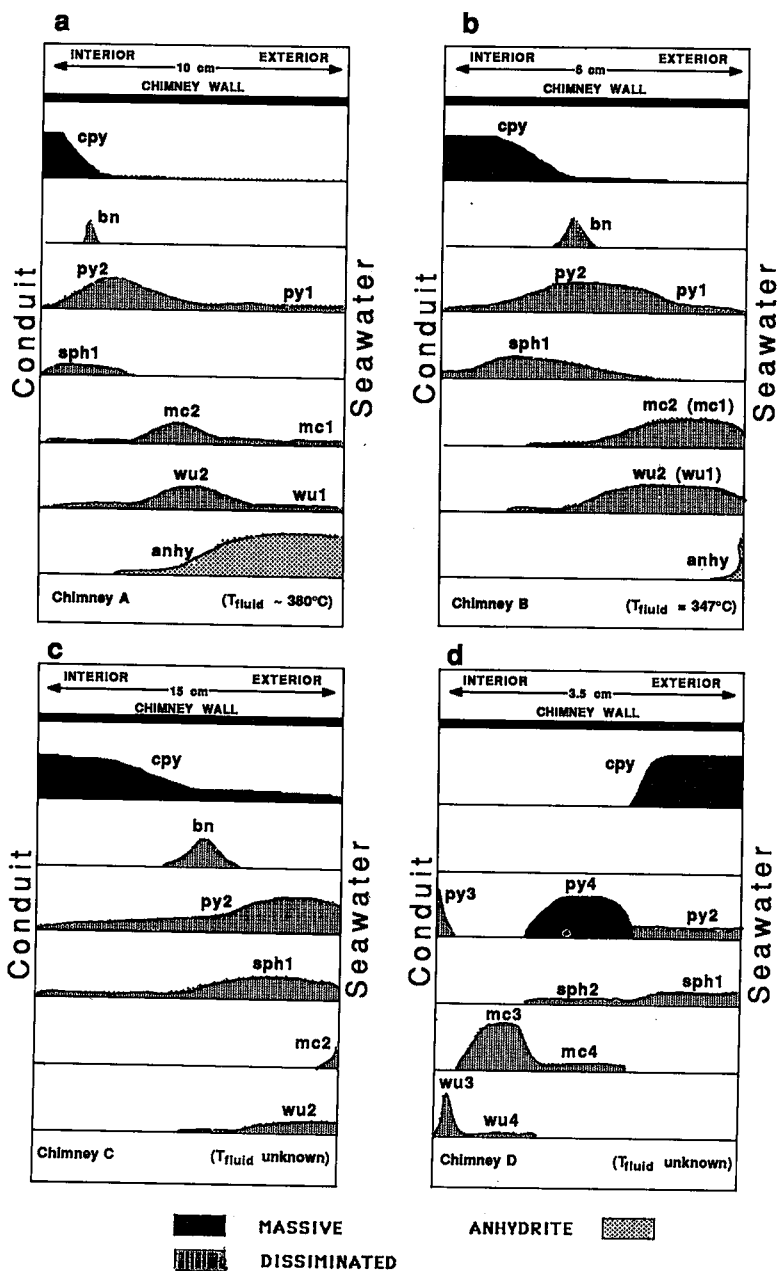
FIG. 3. Representation of the occurrences of major minerals in chimney cross-sections.

up to several mm in length. Cubes of pyrite-2 crystals commonly occur in the inner parts of the Fe- and Zn-rich layers of Chimneys A and B (Fig. 4c,d), but are less abundant in the chalcopyrite-rich zone. Pyrite-2 is the dominant sulfide at the exterior wall in Chimney C, and is the most abundant Fe sulfide at the exterior wall of Chimney D. Most pyrite-2 con-tains inclusions of marcasite and wurtzite (Fig. 4d). The size and textures of some pyrite-2 crystals are reminiscent of colloform marcasite aggregates which commonly form at the outer parts of the Fe- and Zn-rich layers in Chimney B; etch tests of relatively large masses of pyrite-2 show small ($< 10 \mu$m) cubes of pyrite-1 or colloform textures typically observed in

TABLE 1. CHARACTERISTICS OF SULFIDE-TYPES IN CHIMNEYS A-D

TYPE	MORPHOLOGY	GRAIN SIZE(μm)	(%)	COEXISTING PHASES	REPLACEMENT BY
PYRITE-1	subhedral	5-50	10	mc1, wu1, cpy	py2, cpy
PYRITE-2	cubes	70-100	80	mc2, wu2, sph1, cpy	cpy
PYRITE-3	dendritic	10-100	5	wu3	/
PYRITE-4	rounded blades	100-500	5	mc4, sph2	/
MARCASITE-1	anhedral	5-20	10	py1, wu1, cpy	py2, cpy
MARCASITE-2	colloform	50-500	80	wu2, py2, cpy	py2, cpy
MARCASITE-3	a) colloform	80-600	5	wu4, mc4, py4	mc4, py4
	b) needles	10-200	5	mc4, py4	mc4, py4
MARCASITE-4	rounded blades	10-100	5	mc4 , sph2	/
WURTZITE-1	anhedral	5-50	10	py1, mc1, cpy	cpy
WURTZITE-2	colloform	50-300	80	mc2, py2, sph1, cpy	cpy, sph1
WURTZITE-3	elongate crystals	10-100	10	py3	/
WURTZITE-4	hexagonal crystals	<5	<1	mc3	/
SPHALERITE-1	colloform	50-400	95	py2, wu2, cpy	cpy
SPHALERITE-2	anhedral	5-70	5	mc4, py4	/

Footnote: Pyrite-1,-2, marcasite-1,-2, wurtzite-1,-2 and sphalerite-1 occur in active chimneys (A-C); pyrite-2,-3,-4, marcasite-3,-4, wurtzite-3,-4 and sphalerite-1,-2 occur in the extinct chimney D.

marcasite. Pyrite-2 appears to form by inversion from marcasite. It has a distinct anisotropy and displays several kinds of pore spaces, which are typical inversion features (Murowchick & Barnes 1984). Chalcopyrite either engulfs pyrite-2 grains which occur as rounded aggregates, or fills gaps and fracture zones within pyrite-2 and penetrates toward grain interiors. Such processes can lead to atoll textures in pyrite (Craig & Vaughan 1981) as illustrated in Figure 4f.

Pyrite-3 crystals occur along the channelway of Chimney D. They are dendritic, isotropic, and lack inclusions of other sulfides (Fig. 4r). Pyrite-4 forms large (100-500 μm) blades with round edges. It occurs only in the interior of Chimney D, where it forms a solid layer 2 cm wide (Fig. 4j). Pyrite-4 is subhedral and has the strongest anisotropy of any pyrite in the chimneys. Some crystal-growth surfaces of pyrite-4 are slightly curved; such textures appear to have been produced during the growth of precursor twinned marcasite crystals.

The four types of marcasite are listed in Table 1. Marcasite-1 occurs as small (5–20 μm) anhedral grains, coprecipitated with pyrite-1 in the anhydrite-rich zone of Chimney A. Marcasite-2, which consists of large (50–500 μm) anhedral grains with a colloform texture, is common in the outer parts on the Fe- and Zn-rich zone of chimneys A (Fig. 4b) and B, and occurs in minor amounts in the interior walls of active chimneys A, B, and C. Most marcasite-2 grains have undergone replacement by pyrite-2 (Figs. 4c,d).

Marcasite-3 occurs in extinct Chimney D as large (80–600 μm) polycrystalline aggregates, and as needle-shaped crystals (10–200 μm) which grew toward the conduit (Fig. 4o). Marcasite-4 occurs as disseminated grains within the pyrite-4 layer in the interior of Chimney D; marcasite-4 is replaced by pyrite-4 to variable degrees (Figs. 4m,n), and its grain size and crystal habit are usually similar to pyrite-4 blades. In some instances, the interior texture of marcasite-4 resembles the texture of fine-grained aggregates of marcasite-3 (Fig. 4n).

The textural and spacial relationships among the FeS_2 phases indicate that: i) pyrite-1 and marcasite-1 and -2 are the primary FeS_2 phases that formed in the exterior parts of the chimney walls during outward growth; ii) most pyrite-2 crystals formed by transformation of marcasite-1 and -2 and pyrite-1 within the chimney walls (but external to the chalcopyrite layer); iii) some pyrite-2 crystals apparently grew without precursor marcasite or pyrite-1; and iv) marcasite-3 precipitated on the inside of the chalcopyrite wall and recrystallized to marcasite-4, which apparently then transformed to pyrite-4. The degree to which chalcopyrite replaced FeS_2 decreases outward from the chalcopyrite wall in the active chim-

FIG. 4. Photomicrographs illustrating the mineral textures in chimneys A through D under reflected light. A scale bar is displayed at the bottom of each photo: double horizontal bar = 50μm, single horizontal bar = 300μm; py pyrite, cpy chalcopyrite, mc marcasite, wu wurtzite, sph sphalerite, bn bornite, anhy anhydrite. The numbers following py, mc, wu and sph refer to subtypes. The dark grey areas are anhydrite crystals; the black spots are voids.

(a) Characteristic mode of subhedral to euhedral pyrite-1, anhedral marcasite-1, and extremely fine-grained chalcopyrite occurrence within an anhydrite-rich wall (grey matrix).

(b) Precipitation of colloform marcasite-2 and wurtzite-2 with no replacement textures.

(c) Large subhedral to euhedral pyrite-2 crystals that replaced colloform marcasite-2 at the grain interior. The marcasite-2 textures show concentric layering and onset of pyrite replacement as indicated by the color differences within the layers. Small voids are disseminated within the pyrite-2 crystal which is partly replaced by chalcopyrite.

(d) Cubes of pyrite-2 with inclusions of wurtzite-2. Marcasite-2 in the right upper corner is almost entirely replaced by pyrite-2. Chalcopyrite partly replaced both pyrite-2 and wurtzite-2.

(e) Sphalerite-1 with intense chalcopyrite disease. Chalcopyrite replacement proceeded from the rims and growth zones of sphalerite-1 and penetrated towards grain interiors. Pyrite-2 is replaced by chalcopyrite.

(f) Rounded and corroded isolated islands of pyrite-2 and less abundant sphalerite-1 occur in the chalcopyrite-rich zone. Pyrite-2 in center forms atoll textures in the paragenetically later chalcopyrite. Sphalerite-1 is free of chalcopyrite disease.

(g) The field is dominated by elongate pyrrhotite crystals intergrown with chalcopyrite. The textures record intense fracturing of the pyrrhotite with rounded and corroded edges due to replacement by chalcopyrite, and the preservation of small pyrrhotite grains inside pyrite-2 cubes.
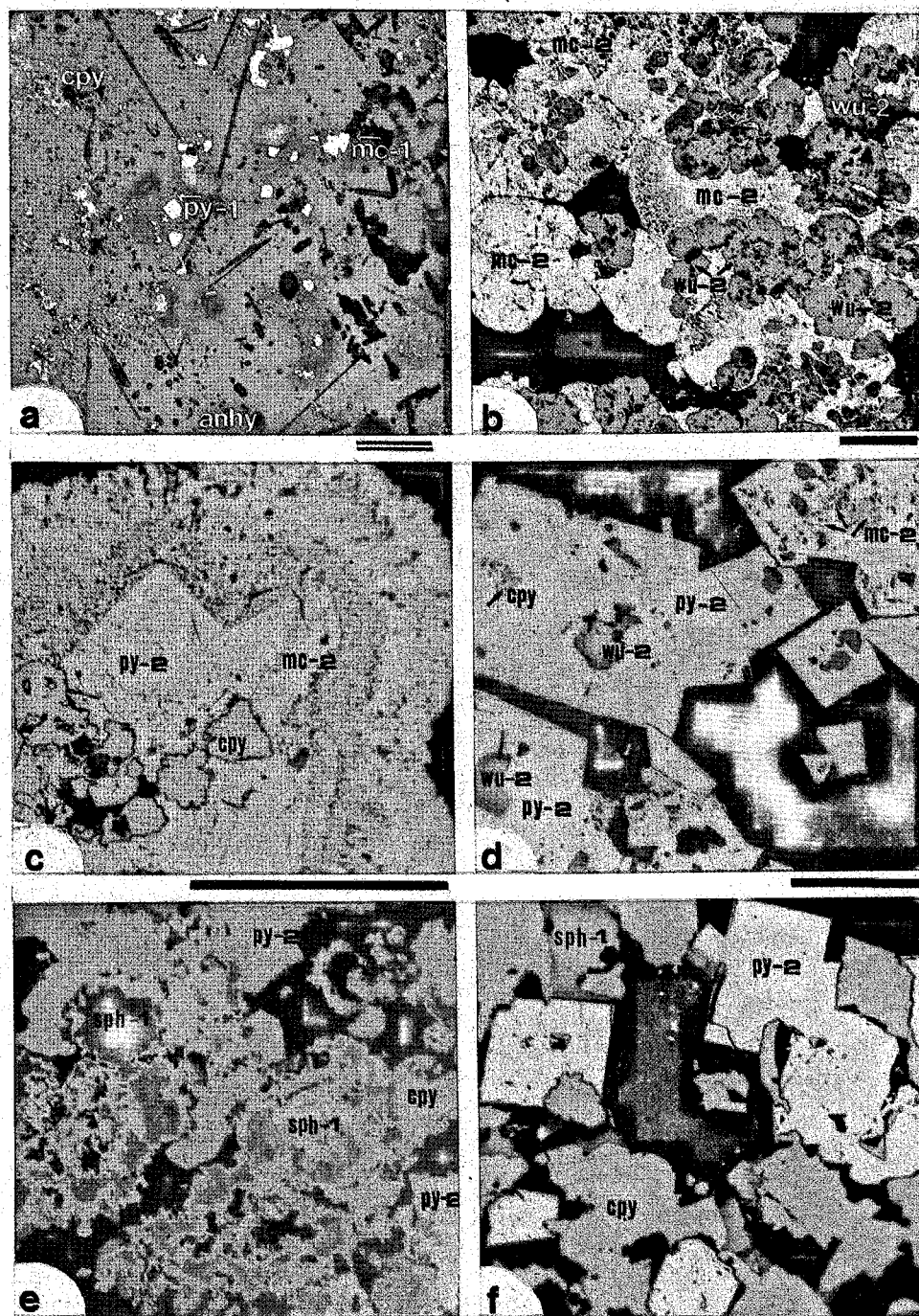
(h) Bornite occurs in the paragenesis with chalcopyrite, pyrite-2 and minor sphalerite-1. Pyrite-2 cubes have been selectively replaced by chalcopyrite (center of field) resulting in a corroded pyrite crystal. Bornite replaced chalcopyrite along cracks. Some chalcopyrite grains are completely replaced by bornite and by later covellite (blue lines).
(i) Cross-section of chimney D.
(j) Enlargement of (i): from right to left the textures record the growth of chalcopyrite by partial replacement of pyrite-2 cubes, a massive layer of pyrite-4 blades, the inclusion of anhedral sphalerite-2 within pyrite-4 blades, large colloform marcasite-3 aggregates, and the occurrence of subhedral wurtzite-3.
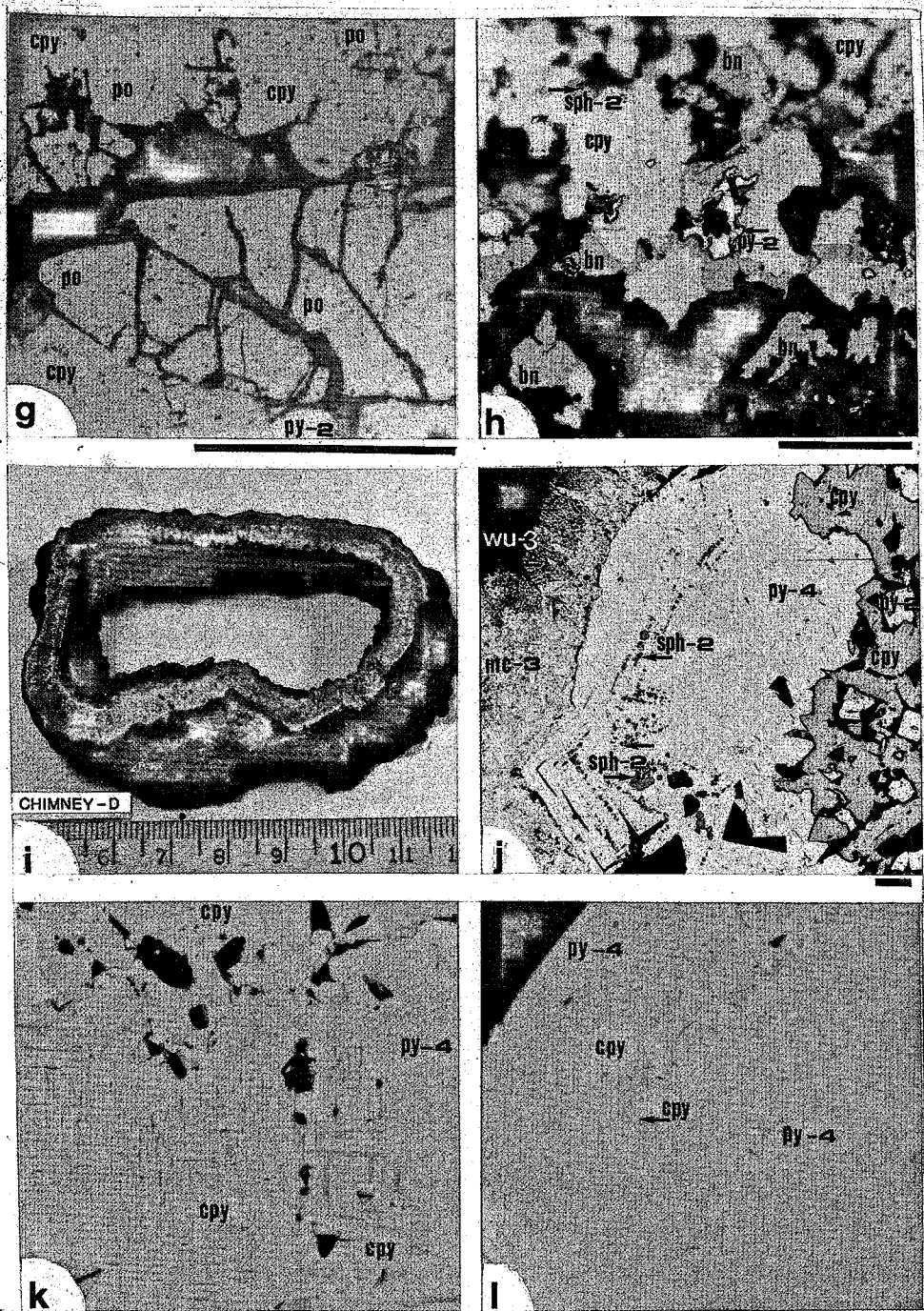
(k) Intergrowth of pyrite and chalcopyrite: the pyrite-4 blades include chalcopyrite lamellae in orthogonal and triangular arrays. Pyrite-4 blades are not replaced by chalcopyrite, but chalcopyrite lamellae are replaced by pyrite-4.
(l) Highly rounded pyrite-4 blade with chalcopyrite lamellae occuring perpendicular to the growth surface of pyrite-4.
(m) Selective replacement of a marcasite-4 grain by pyrite-4 as indicated by the same interference color of the marcasite-4 remnants. Pyrite-4 blades form a massive layer. Pyrite-2 at the left upper corner is replaced by chalcopyrite.
(n) A large marcasite-3 grain partly replaced from the outside by pyrite-4 shows a series of sphalerite-2 inclusions. The interior has a fine-grained texture. Pyrite-4 blades at the lower right are highly anisotropic.
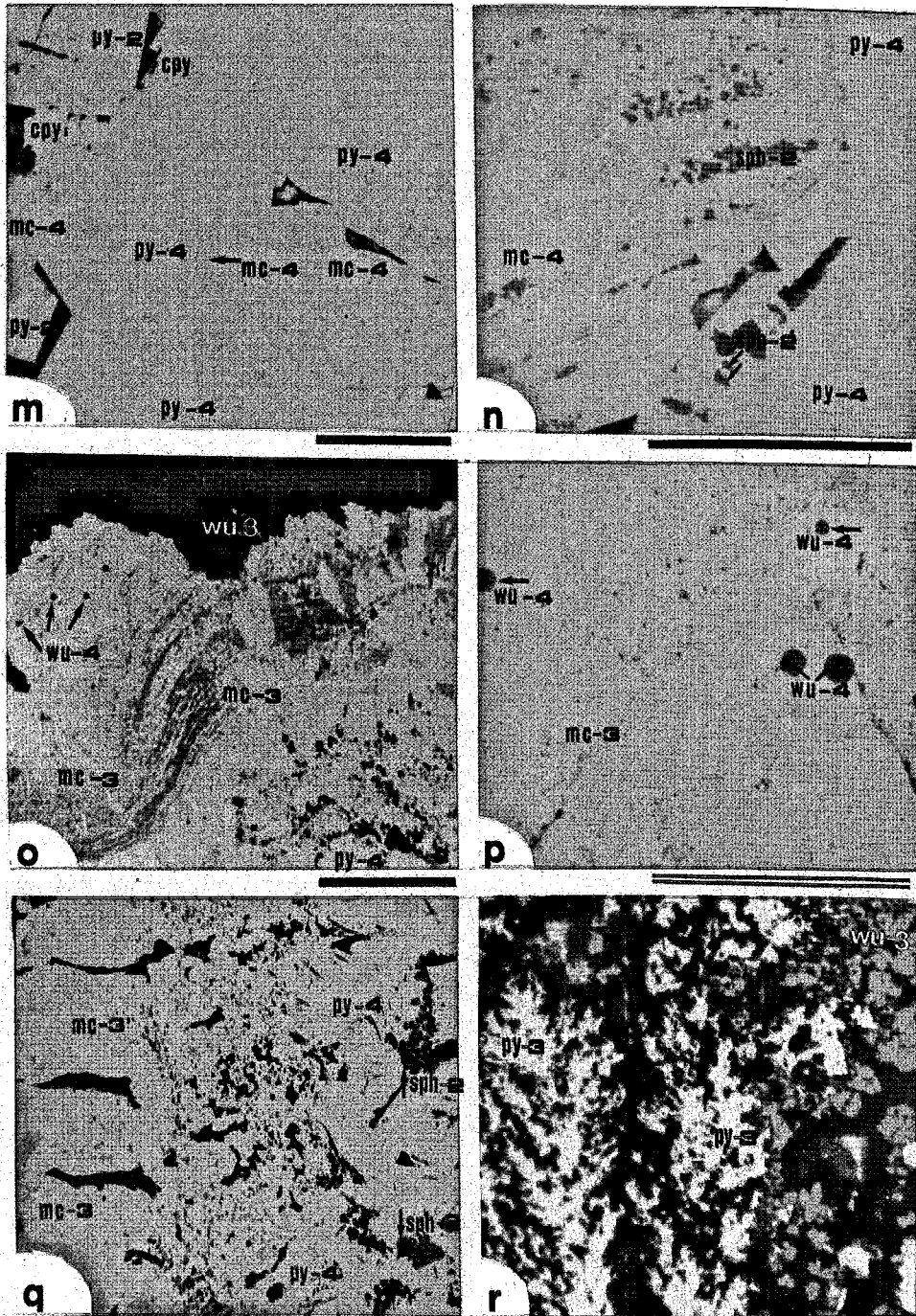
(o) Marcasite-3 is a combination of fine-grained colloform aggregates and elongate crystals. The many void spaces indicate a high porosity of marcasite-3. Some marcasite-3 shows inclusions of extremely small wurtzite-4. Wurtzite-3 occurs outside the marcasite-3 and shows no textural relationship to marcasite-3.
(p) Enlargement of (o): wurtzite-4 with a hexagonal crystal habit occurs in a matrix of marcasite-3.
(q) Marcasite-3 and pyrite-4 in nearly monomineralic zones; many voids occur at the interface of both zones.
(r) The textures record the growth of dendritic pyrite-3 which occurs in the paragenesis with subhedral wurtzite-3. Some wurtzite grains are encrusted by dendritic pyrite.

TABLE 2. MICROPROBE ANALYSES

a) FeS$_2$

FeS$_2$ - TYPE	# of GRAINS	CHIMNEY	Cu [wt%]	Zn [wt%]	Co [wt%]
PYRITE-1	21	A	0.05 - 0.10	0.08 - 0.20	<0.02
PYRITE-2	25	A, B, C	0.05 - 0.13	0.10 - 0.23	<0.02
PYRITE-3	17	D	0.35 - 0.55	<.05 - 0.06	<0.02
PYRITE-4	15	D	0.05 - 0.09	<.05 - 0.21	<0.02
MARCASITE-2	25	B, C	<.05 - 0.05	0.05 - 0.37	0.06 - 0.11
MARCASITE-4	25	D	0.10 - 0.15	0.09 - 0.28	0.04 - 0.10

b) ZnS

ZnS - TYPE	# of GRAINS	CHIMNEY	FeS [mol%]	Cu [wt%]	Cd [wt%]
WURTZITE-2	80	B, C	2.9 - 9.6	0.05 - 2.10	0.19 - 0.33
WURTZITE-3	23	D	14.5 - 21.5	0.21 - 0.51	0.09 - 0.27
SPHALERITE-1	10	B, C	3.5 - 15.2	0.10 - 2.05	—

c) BORNITE

Cu$_5$FeS$_4$ in	Zn [wt%]	
CHIMNEY A	0.05 1.03 3.04	toward exterior wall
CHIMNEY B	1.40 3.37 3.97	toward exterior wall

Detection limits are: 0.05% for Fe, Cu, Zn, and 0.03 for Co

neys. FeS$_2$ phases inside the chalcopyrite wall of Chimney D (marcasite-3, and -4, and pyrite-3 and -4) are free of chalcopyrite replacement. The ratio of pyrite-2 to (pyrite-1 + marcasite-1 + marcasite-2), which generally increases inward in the chimney walls, is utilized in this study as an indicator of the maturity of chimneys, and increases from Chimneys A through D.

The only pyrrhotite grains observed are in the innermost layer at the orifice of Chimney C, occuring as replacement remnants in pyrite-2 and chalcopyrite, or as corroded remnants (Fig. 4g). This indicates that pyrrhotite, precipitated directly from the hot fluids, can survive only when engulfed by less soluble sulfides. The mole fraction of FeS in 21 grains of pyrrhotite was found to be 0.93 ±0.02 by electron-probe analyses. These N_{FeS} values, together with the $N_{FeS} - T - fS_2$ relationships established by Barton & Toulmin (1964), suggest the minimum fluid temperature of ~270°C.

Microprobe analyses of both pyrite and marcasite are presented in Table 2. There is little difference in the Cu, Zn, and Co contents in Fe sulfides of different generations, except for pyrite-4. Pyrite-4 crystals are distinctly higher in Cu (0.35–0.55 wt.% versus <0.15 wt.%), and generally lower in Zn (<0.06 wt.% versus 0.05–0.37 wt.%).

Zinc sulfides

Four types of wurtzite (Table 1) and two differ-

ent forms of sphalerite have been distinguished microscopically. Wurtzite-1 occurs as small (5–50 μm) grains in association with pyrite-1 and marcasite-1 within the anhydrite-rich zone of Chimney A. It is not observed in the extinct chimney. Wurtzite-2 forms large (50–300 μm), colloform aggregates (Fig. 4b), and is the most abundant type of wurtzite in the Fe- and Zn-rich layer in the active chimneys. It also occurs with large (50–400 μm) sphalerite-1 aggregates in interiors of active chimneys. The original crystal habit in most cases is masked by partial replacement by chalcopyrite (*i.e.*, the "chalcopyrite disease" of Barton 1978).

Wurtzite-3 and -4 form subhedral and euhedral crystals, and occur at the inner wall of extinct Chimney D. Wurtzite-3 occurs as large (10–100 μm) crystals which line the conduit and may be encrusted by dendritic pyrite-3 (Fig. 4r). Wurtzite-4 is present as smaller (<5 μm), hexagonal grains enclosed by marcasite-3 (Figs. 4o,p).

Colloform sphalerite-1 is present in all chimneys. Subhedral sphalerite-2 occurs only at the interior wall of the extinct chimney, normally as relatively small (5–70 μm) grains along crystal surfaces of pyrite-4 and within marcasite-4 (Figs. 4j,n).

The textural and spatial relationships among the ZnS phases indicate that: i) wurtzite-1 is the primary ZnS phase in the outermost parts of the active chimneys; ii) wurtzite-2 occurs toward the interior; iii) both wurtzite-1 and -2 appear to be converted to sphalerite-1, although some primary sphalerite-1 crystals are found at the interior of the active chimneys; and iv) wurtzite-3 and -4 are primary phases inside the chalcopyrite wall of the extinct chimney; both appear to convert to sphalerite-2 (as suggested by the crystal habit of some sphalerite-2). The degree to which wurtzite-1 and -2 and sphalerite-1 are replaced by chalcopyrite decreases outward from the chalcopyrite wall in the active chimneys; ZnS phases inside the chalcopyrite wall of the extinct chimney (wurtzite-3 and -4 and sphalerite-2) are not replaced by chalcopyrite. The ratio of sphalerite-1 to (wurtzite-1 + wurtzite-2) was used as an indicator of the maturity of chimneys. This ratio increases from chimneys A through D. The FeS content in wurtzite and sphalerite ranges from 2.9 to 21.5 mole % in the 113 grains analyzed by electron microprobe, indicating that some ZnS crystals with FeS contents >20.5 mole % must have been in equilibrium with pyrrhotite rather than with pyrite (Barton & Toulmin 1966), although pyrrhotite is rare in the chimney structure. The transformation and replacement processes among the Fe and Zn sulfides are illustrated in Figure 5.

Cu–Fe sulfides

Chalcopyrite (>90 vol.% of total Cu sulfides) occurs as anhedral, 5–500 μm grains which com-

monly line inner walls of active chimneys and the exterior walls of the extinct chimney. Minor (<5%) replacement of Fe and Zn sulfides by chalcopyrite occurs along grain boundaries in the exterior walls of active chimneys; replacement is nearly complete in the conduit walls of the active chimneys.

Bornite with minor digenite and covellite is developed between the chalcopyrite-rich and Fe- and Zn-rich zones of the active chimneys, as well as at the exterior of the extinct chimney adjacent to the chalcopyrite layer. Bornite occurs as small (<5 μm) blebs within pyrite-2, as irregular patches on the outside of pyrite-2 and chalcopyrite grains (Fig. 4h), and as narrow layers that cut chalcopyrite associated with either pyrite-2 or sphalerite-1. Much of the bornite is replaced by covellite and digenite, except where the bornite occurs as isolated blebs in pyrite-2, suggesting that bornite is earlier than covellite and digenite. Chalcopyrite occurring as the inner lining of active chimneys, and as the exterior wall of the extinct chimney, is Zn-poor; chalcopyrite associated with bornite contains up to 3 wt.% Zn. Variations in the Zn contents of bornite are given in Table 2c.

Unique ore-textures, which we term "chalcopyrite lamellae" in pyrite-4 blades (Figs. 4k,l) are developed as groups at the interface with the chalcopyrite-rich zone in the extinct Chimney D. Within each group the lamellae are almost identical in size, although they range from 5 to 100 μm among different groups. They occur in orthogonal and triangular arrays and also perpendicular to growth surfaces of pyrite; some are also found in marcasite-4. Phase relations in the Cu–Fe–S system (Barton 1973, Cabri 1973, Crerar & Barnes 1976) indicate that such textures cannot be caused by exsolution processes within pyrite.

The textural relationships between isocubanite and chalcopyrite, where isocubanite crystallized at $T \geq 210°C$ and exsolved chalcopyrite during quenching (Cabri et al. 1973, Dutrizac 1976), are strikingly similar to the "chalcopyrite lamellae" in pyrite-4 blades. We therefore suggest that precipitation and growth of isocubanite took place at the interior of Chimney D at $T \geq 210°C$, and that the isocubanite quenched to much lower temperatures to preserve the cubic form. If later hydrothermal fluids replaced the isocubanite preferentially to the chalcopyrite to form FeS_2 (marcasite-4 and pyrite-4), the "chalcopyrite lamellae" in the FeS_2 can be explained. This implies that the chalcopyrite layer in the outer wall of extinct Chimney D was formed earlier than the inner marcasite-4 and pyrite-4 layers. Because marcasite generally inverts to pyrite at $T \geq \sim200°C$ (Murowchick & Barnes 1986b), the preservation of marcasite in the interior of Chimney D suggests that the temperatures of hydrothermal fluids decreased from the earlier Cu–Fe sulfide stage (>210°C) to the later FeS_2 stages (<200°C) in extinct Chimney D. That is, clogging of the chimney conduit took place
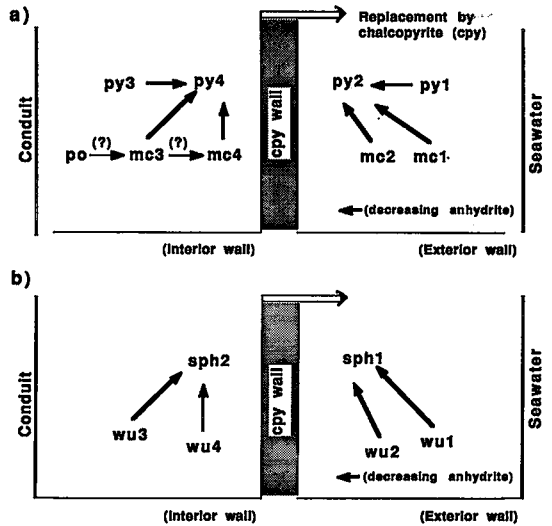
FIG. 5. Diagram illustrating temporal and spatial relationships of several types of (a) FeS_2, and (b) ZnS in the active, and in the extinct chimney. The phases are arranged by relative distance from the chalcopyrite wall. The arrows point in the direction of phase transformation. FeS_2 and ZnS occurring outside of the chalcopyrite wall are observed in the active chimneys (A–C); in the extinct Chimney D, FeS_2 and ZnS occur inside the chalcopyrite wall.

during declining thermal activity, whereas the outward growth of sulfide zones in the active chimneys occurred during intensifying thermal activity.

DISCUSSION

Chimney-growth model

Chimneys have growth histories which are often extremely complex, involving multiple stages of mineralization, heating, cooling, and the sealing or opening of new vents. Only within the simplest case does chimney growth occur around a single vent orifice with a systematic progression of mineralogical zones. However, consistent paragenesis and spatial relationships of sulfides and anhydrite in the 27 chimney samples suggest that the process of mineralization was similar at all locations; differences among chimney mineralogy and zoning may reflect variations in maturity and preservation of the chimneys, as well as the thermal and compositional history of hydrothermal fluids.

Our observations have led us to define 8 mineralogical zones in an idealized chimney (Table 3, Fig. 6). None of the chimneys exhibits a complete sequence, and the zone thicknesses vary considerably. The term "mineralogical facies" may be more accurate than "mineralogical zones", because each

Table 3.　Characteristic Mineral Assemblages and Spatial Relationship of Mineral Facies

Chimney Sample	FACIES Diagnostic Mineral Phases									
	8	7	6	5	4	3	2	1		
	wu3 py3	mc3 wu4	py4 mc4 sph2 cpy	cpy iss py2 sph1 wu2 po	cpy bn py2 sph1 wu2	py2 sph1 wu2 cpy py1 mc2 anhy	mc2 wu2 py1 mc1 cpy anhy	anhy py1 wu1 mc1 cpy	Increasing Abundance	
D										Increasing Maturity
C										
B										
A										

Interior ←　Chimney Wall　→ Exterior

mineralogical zone is characterized by a distinct mineral assemblage and textures, and because the mineralogical zones are not stationary during the history of a chimney; they may migrate outward or inward in a chimney, be replaced by other mineralogical zones, or be dissolved away by later hydrothermal fluids or by local seawater. The use of "mineralogical facies", rather than "zones", has been justified by Eldridge *et al.* (1983) in their mineralogical study of Kuroko and other volcanogenic massive sulfide deposits.

The 8 mineralogical zones (facies), aligned from the exterior to the interior in an idealized chimney, have the following characteristics:

Zone 1. A porous framework of anhydrite crystals with <5 vol.% of disseminated sulfides (pyrite-1 + marcasite-1 + wurtzite-1 ± chalcopyrite). Facies-1 minerals are very fine grained, suggesting that they formed rapidly by mixing of hot fluids and cold seawater.

Zone 2. Aggregates of marcasite-2 and wurtzite-2 (up to 80 vol.%) with minor pyrite-1, marcasite-1 and relicts of anhydrite. Some facies-2 minerals appear to have formed as recrystallization products of facies-1 minerals; the others appear to be direct precipitates from hydrothermal fluids within the pore spaces in zone 1.

Zone 3. Coarse-grained pyrite-2 ($\geq$ 60 vol.%), sphalerite-1, and wurtzite-2 with minor amounts of pyrite-1 and marcasite-2. All Fe–Zn phases are partly ($\sim$30%) replaced by chalcopyrite. Facies-3 minerals appear to be mostly the recrystallization products of facies-2 sulfides, but some may have precipitated directly from hydrothermal fluids.

Zone 4. Sulfur-rich Cu sulfides (bornite ± covellite ± digenite) with chalcopyrite, pyrite-2, and sphalerite-1. Facies-4 minerals appear to be the

products of reaction between facies-5 sulfides and later, cooler fluids.

Zone 5. Massive, coarse-grained chalcopyrite intergrown with isocubanite. Pyrite-2 and sphalerite-1 (± wurtzite-2) are also present within the pore space (10–20 vol.%). Facies-5 minerals appear to be replacement products of facies-3 minerals.

Zone 6. A massive pyrite layer composed primarily of aggregates of pyrite-4 blades with relicts of marcasite-4 ($\sim$10 vol.%). Sphalerite-2 occurs as inclusions in pyrite-4 and marcasite-4, and as overgrowth on the FeS_2 phases.

Zone 7. Marcasite-3 with minor (<0.1 vol.%) hexagonal wurtzite-4 inclusions.

Zone 8. Subhedral wurtzite-3 crystals with overgrowths of dendritic pyrite-3. Zones 6, 7, and 8 are restricted to the interior of extinct Chimney D. Facies-7 and -8 minerals appear to have grown inward from a chimney wall composed of facies-5 minerals; facies-6 sulfides appear to be the recrystallization products of facies-7 and -8 minerals.

Our interpretation of the change with time in the widths and the positions (relative to the chimney conduit) of the 8 mineralogical zones (facies) in an idealized chimney is illustrated schematically in Figure 6. Horizontal lines in Figure 6 represent the order of mineralogical zones which a fluid of a given stage of hydrothermal activity might encounter during its migration from the channelway, through the chimney wall, to the surrounding seawater. For example, the fluid discharged at time C may encounter successively facies $5 \rightarrow 4 \rightarrow 3 \rightarrow 2 \rightarrow 1$ during migration outward. Therefore, a horizontal line is equivalent to the representation of a cross-section of a chimney wall at a given stage of its growth history. Horizontal lines A, B, C, and D represent the cross-sections of chimneys A, B, C, and D, respectively. Their relative positions with respect to the y (time) axis imply that these chimneys represent different stages of the development of an ideal chimney.

Our chimney-growth model (Fig. 6) incorporates the following major concepts concerning the growth and preservation of chimney structures:
1) The chimneys grow outward when the rate of precipitation on the exterior wall of facies-1 minerals (anhydrite + wurtzite-1 + pyrite-1) exceeds that of mineral dissolution by the surrounding seawater. During and after waning of hydrothermal activity, chimneys are dissolved by cold seawater and diminish in size because seawater is undersaturated with respect to the chimney sulfides and sulfates. Dissolution continues until the chimneys are covered by sediments or oxidized to ferric oxides (or both).
2) During the outward growth of chimneys, the earlier formed minerals on the inner wall are continuously dissolved by later hydrothermal fluids, because the fluids are initially undersaturated with respect to the chimney minerals. The larger conduit
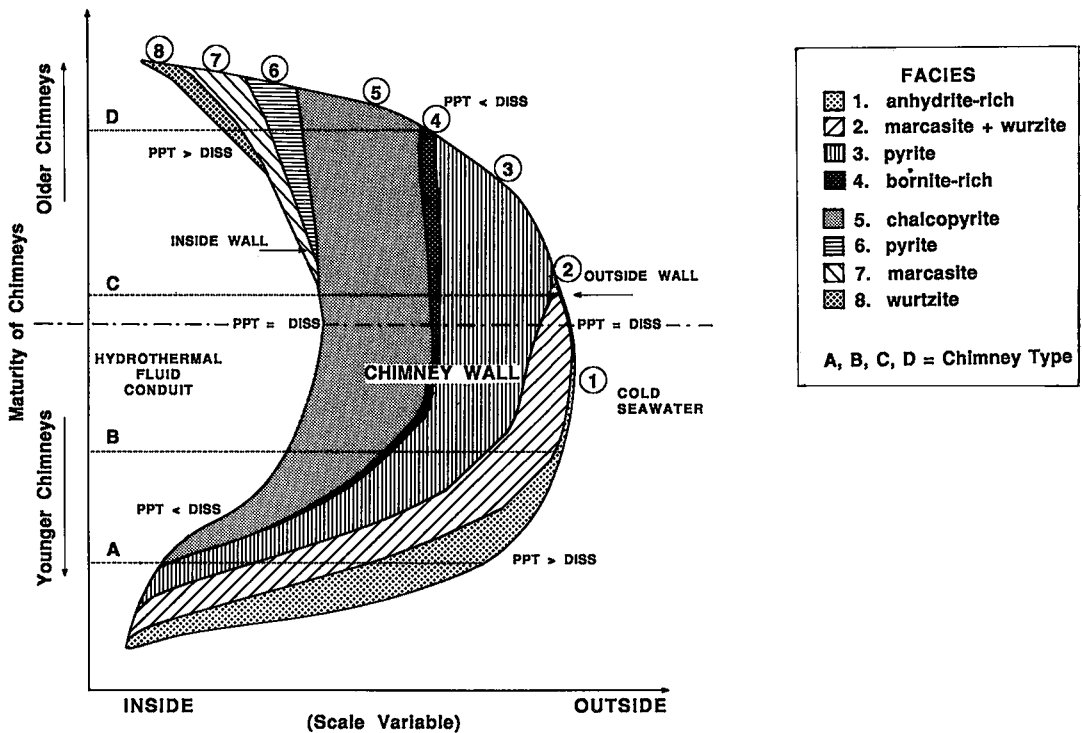
FIG. 6. Schematic diagram illustrating the growth and dissolution history of a model (ideal) chimney. The spatial relationships of different mineralogical zones or facies of chimneys A, B, C and D are compared. Maturity of the chimneys is indicated by the vertical axis. The horizontal axis shows the relative distance from the chimney conduits to the exterior walls, which simply reflects the width of the chimney wall. Chimney A is interpreted as the least mature and Chimney D as the most mature. PPT: mineral precipitation rate; DISS: mineral dissolution rate. See text for further explanation of the model.

diameter of Chimney C relative to Chimney A (~7 cm *versus* ~3 cm) suggests that the rate of mineral dissolution at the inner wall exceeded that of mineral precipitation in the active chimneys.

3) The hydrothermal fluids that migrate through the chimney wall react with the earlier minerals, dissolving them or transforming them (or both) successively to the mineral assemblages that are more stable at higher temperatures (*e.g.*, facies $1 \rightarrow 2 \rightarrow 3 \rightarrow 5 \rightarrow 4$). Some of the dissolved materials from the interior zones may reprecipitate in the pore space of the outer zones or on the exterior surface. That is, each mineralogical zone contains the old materials (sulfur and metals), which were fixed there as earlier minerals, as well as the younger materials that were introduced there by later hydrothermal fluids. The proportion of older to younger materials increases toward the outer zone; the outermost zone (anhydrite-rich zone) contains the highest proportion of the oldest materials. This is in good agreement with sulfur isotope data obtained in these chimney zones (Bluth & Ohmoto 1988). The chimney-growth processes are, therefore, analogous to the migrating reaction front

during skarn mineralization, with a major difference that the material replaced is anhydrite instead of limestone.

4) Conduits fill when the rate of mineral precipitation on the interior wall exceeds that of mineral dissolution during the waning stage of hydrothermal activity. Some of these minerals transform to more stable phases during interaction with later fluids. For example, facies-6 minerals (pyrite-4) of Chimney D are probably the products of transformation of facies-7 and -8 minerals.

Chemical processes of chimney growth

Anhydrite. The precipitation of anhydrite ($CaSO_4$) during the mixing of hydrothermal fluid and cold seawater has been noted by many investigators (Spiess *et al.* 1980, Ohmoto *et al.* 1983). The Ca^{2+} in anhydrite is derived largely from the hydrothermal fluids; sulfur isotope evidence indicates that the SO_4^{2-} is derived from local seawater (Kusakabe *et al.* 1982).

The anhydrite of facies 1 is continuously dissolved from chimney interiors by later hydrothermal fluids

because these fluids are nearly sulfate-free (*e.g.*, Edmond *et al.* 1979, Styrt *et al.* 1981, Von Damm *et al.* 1983, Ohmoto *et al.* 1983). The anhydrite is also dissolved from the chimney exterior by cold seawater because seawater is undersaturated with respect to anhydrite.

Fe sulfides. High-temperature hydrothermal fluids developed in basaltic rocks are typically at or near the saturation conditions of both pyrrhotite and pyrite; they typically have H_2S contents of 10^{-3} – 10^{-1} moles/kg H_2O and ΣSO_4^{2-} contents of $<10^{-3}$ moles/kg H_2O at $T = 250$–$400°C$ (*e.g.*, Edmond *et al.* 1979, Styrt *et al.* 1981, Von Damm *et al.* 1983, Von Damm 1988, Ohmoto 1988). It has been demonstrated experimentally by Murowchick & Barnes (1986a) that simple cooling of such fluids results in precipitation of pyrrhotite (FeS), rather than pyrite or marcasite (FeS_2):

$$Fe^{2+} + H_2S \rightarrow FeS + 2H^+ \qquad (1)$$
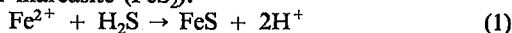
Thus, simple cooling of the hydrothermal fluids can explain the presence of pyrrhotite in the black smoke (*e.g.*, Haymon & Kastner 1981) and also in the interior of Chimney C.

Formation of FeS_2 minerals requires polysulfide species, such as H_2S_2 and HS_2^- (Murowchick & Barnes 1986b):

$$Fe^{2+} + H_2S_2 \rightarrow FeS_2 + 2H^+ \qquad (2)$$
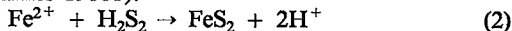
Since the equilibrium concentration of H_2S_2 (and other polysulfide species) in hydrothermal fluids is many orders of magnitude less than that of H_2S (*e.g.*, Murowchick & Barnes 1986b), a significant quantity of FeS_2 would form only if polysulfide species are continuously generated *at the depositional site* from more abundant sulfur species, such as H_2S in the hydrothermal fluids and/or SO_4^{2-} in seawater (and anhydrite which formed from seawater SO_4^{2-}). Several possible mechanisms exist for the generation of polysulfide species in the depositional environment of the chimneys (Ohmoto 1988):
(i) Oxidation of hydrothermal H_2S by dissolved O_2 in seawater:

$$2H_2S + \tfrac{1}{2}O_2 \rightarrow H_2S_2 + H_2O \qquad (3)$$

(ii) Oxidation of hydrothermal H_2S by diffusive loss of hydrothermal H_2:

$$2H_2S \rightarrow H_2S_2 + H_2(\uparrow) \qquad (4)$$

(iii) Reaction between hydrothermal H_2S and seawater SO_4^{2-}:

$$7H_2S + 2H^+ + SO_4^{2-} \rightarrow 4H_2S_2 + 4H_2O \qquad (5)$$

(iv) Reduction of seawater SO_4^{2-} by hydrothermal H_2:

$$7H_2 + 4H^+ + 2SO_4^{2-} \rightarrow H_2S_2 + 8H_2O \qquad (6)$$
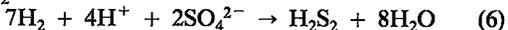
The relative importance of the above four mechanisms of polysulfide generation depends partly on the relative abundances of H_2S, O_2, H_2, H^+ and SO_4^{2-} in the hydrothermal fluids and seawater. For example, if the mixing seawater contained only $\sim 10^{-6}$ m of dissolved O_2 or if the hydrothermal fluids contained only $\sim 10^{-6}$ m of H_2, the amounts of H_2S_2

(and FeS_2) produced from reactions (3) and (4) would not exceed $\sim 10^{-6}$ m. However, the O_2 content of normal (oxic) seawater in deep oceans ($\sim 10^{-3.5}$ m; Drever 1982) and the H_2 content of the EPR fluids ($\sim 10^{-3.5}$ m; Welhan & Craig 1983, Ohmoto 1988) are less than the H_2S content of the hydrothermal fluids (10^{-3} – 10^{-1} m), but they are sufficiently high to become quantitatively important in the formation of FeS_2 via reactions (3) and (4). Normal seawater contains large amount of SO_4^{2-} ($\sim 10^{-1.7}$ m; Drever 1982). The rates of reactions (3) – (6) appear to increase rapidly with increasing temperature ($T \geq 150°C$), and with decreasing pH (≤ 4; Ohmoto 1988).

During the rapid cooling of hydrothermal fluid (from $\sim 350°C$ to $\sim 2°C$ in $\sim$ seconds) due to mixing with cold seawater above the chimneys, the reaction rates of (3)–(6) are probably much slower than the reaction rate of (1), explaining why pyrrhotite, rather than FeS_2 minerals, is the dominant Fe-sulfide phase in the black smoke (Ohmoto 1988). If fluid mixing occurs slowly within warm chimney structures, formation of polysulfide species (and FeS_2 minerals) via reactions (3) through (6) may be facilitated.

The presence of different types and proportions of marcasite and pyrite in the different chimney zones suggests that more than one mechanism of polysulfide generation occurs in the chimney environment. Precipitation of marcasite apparently requires acidic conditions (pH $< \sim 4.5$ at $T < \sim 200°C$), whereas pyrite precipitation is favored at higher pH conditions (Murowchick & Barnes 1986b, Goldhaber & Stanton 1987). The fact that the pH of the EPR fluids is typically $< \sim 4.5$ (*e.g.*, at $21°N$: Von Damm *et al.* 1983, Campbell *et al.* 1988; at 11–$13°N$: Bowers *et al.* 1988), and that marcasite is the dominant FeS_2 phase in the outermost zone of active chimneys (marcasite-1 in zone 1) and in the innermost zone of the clogged chimney (marcasite-3 in zone 7), suggests that the less abundant marcasite phases formed primarily by reactions (3) or (4) (or both). The more abundant marcasite-2 and -4, which occur mostly in the interior parts of the chimneys (zones 2, 3, and 6), may have been formed by reaction (5), *i.e.*, the reaction between hydrothermal H_2S and SO_4^{2-} that is constantly supplied by the dissolution of earlier anhydrite by warmer hydrothermal fluids. Primary pyrite phases (pyrite-1, pyrite-3, and some pyrite-2) in the chimneys may have formed because the hydrothermal fluids were neutralized by dissolution of earlier anhydrite and sulfide minerals. Continuous heating of the chimney wall by later fluids, together with the tendency of increasing pH of fluids inside the chimney structure, are probably responsible for the conversion of marcasite and primary pyrite phases to larger grained pyrite phases (pyrite-2 and -4).

ZnS. The observed trend of increasing wurtzite/sphalerite ratio from the chalcopyrite wall both to the outside walls (in the active chimneys) and inside wall (extinct chimney) as illustrated in Figure 5b suggests that the rate of nucleation is an important factor controlling the ZnS mineralogy: rapid nucleation caused by quenching apparently leads to the formation of wurtzite, whereas slower nucleation in warmer environments (*e.g.*, chimney-wall interiors) leads to the precipitation of sphalerite.

Chalcopyrite. Precipitation of chalcopyrite from the hydrothermal fluid bearing Cu^+, Fe^{2+} and H_2S requires an oxidation mechanism:

$$Cu^+ + Fe^{2+} + 2H_2S + \tfrac{1}{4}O_2 \rightarrow CuFeS_2 + 3H^+ + \tfrac{1}{2}H_2O \qquad (7)$$
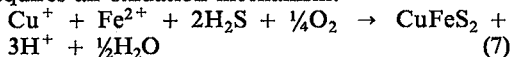
Slow rates of oxidation reactions during rapid mixing of hot fluids and cold seawater (see above discussion on pyrite) explain why chalcopyrite is not abundant in the black smoke. In contrast, the availability of various oxidation mechanisms in the chimney environment, and the prolonged contact of the hydrothermal fluids with these oxidants, explain the occurrence of a small amount of chalcopyrite, especially in the anhydrite-rich zone 1.

Chalcopyrite in facies 5 appears to have formed largely by reaction of a Cu- and Fe-bearing hydrothermal fluid with pre-existing (*i.e.* facies 1–3) ZnS or FeS_2 minerals (or both) through reactions such as:

$$Cu^+ + Fe^{2+} + H^+ + \tfrac{1}{4}O_2 + 2ZnS \rightarrow CuFeS_2 + 2Zn^{2+} + \tfrac{1}{2}H_2O \qquad (8)$$

$$Cu^+ + FeS_2 + \tfrac{1}{2}H_2O \rightarrow CuFeS_2 + H^+ + \tfrac{1}{4}O_2 \qquad (9)$$
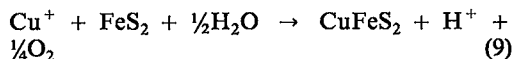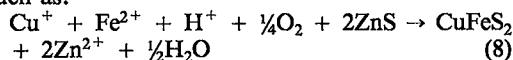
The combination of reactions (8) and (9) represents replacement of both FeS_2 and ZnS by chalcopyrite:

$$2Cu^+ + Fe^{2+} + 2ZnS + FeS_2 \rightarrow 2CuFeS_2 + 2Zn^{2+} \qquad (10)$$

which is manifest as chalcopyrite disease. The stoichiometry of reaction (10) implies that ZnS is consumed at a faster rate than FeS_2 during replacement by chalcopyrite and thus can explain the trend of increasing FeS_2/ZnS ratios inward in the chimney structure. The Zn released by reaction (10) may partly reprecipitate in zones 2 and 1.

Reactions (8)–(10) suggest that the formation of chalcopyrite and dissolution of FeS_2 may cease once all the ZnS is consumed, unless a reduction mechanism exists within the chimney (see reaction 9). This is probably the reason why the nearly monomineralic pyrite zone (zone 3) is developed between the inner monomineralic chalcopyrite zone (zone 5) and the outer zone rich in Zn and Fe sulfides (zone 3). Therefore, more mature chimneys would tend to have higher Cu/Fe, Cu/Zn, Fe/Zn, and Σsulfide/anhydrite ratios, and also develop more monomineralic zones.

The "replacement" texture of chalcopyrite by pyrite observed between zones 5 and 6 in extinct Chimney D (Fig. 4k) may be a reversal of reaction (9). Note that the direction of reaction (9) depends on the concentration of Cu^+ in the fluids, as well as on *T*, pH, and the availability of redox mechanisms; lower concentration of Cu^+ in later lower temperature fluids and the availability of oxidation mechanisms may have promoted pyrite formation over chalcopyrite.

S-rich Cu sulfides. Fluids in equilibrium with chalcopyrite tend to move into the stability fields of S-rich Cu sulfides (*e.g.*, bornite, covellite) during cooling (Ohmoto *et al.* 1983). Given a sufficient supply of H_2S, an oxidation mechanism, and a temperature gradient across the chimney wall, the following reactions tend to proceed to the right:

$$5CuFeS_2 + 2H_2S + O_2 \rightarrow Cu_5FeS_4 + 4FeS_2 + 2H_2O \qquad (11)$$

$$Cu_5FeS_4 + 3H_2S + \tfrac{3}{2}O_2 \rightarrow 5CuS + FeS_2 + 3H_2O \qquad (12)$$
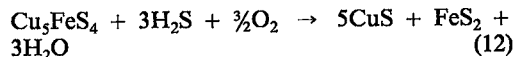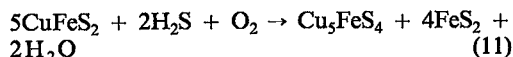
These reactions can explain the occurrence of a S-rich Cu sulfide assemblage (facies 4) in the outer parts of the chalcopyrite-rich zone 5.

SUMMARY

Important observations and suggestions made in this study are summarized below:

1) Variations in the mineralogy, texture, and zoning of 27 chimneys from 11 vent sites at 11° and 13°N on the EPR are represented by 3 active and 1 extinct chimneys.

2) The three active chimneys show the common zoning: an anhydrite-rich outer zone, a transition zone rich in Fe and Zn sulfides, and a chalcopyrite-rich innermost zone, although the thickness of each zone varies among the chimneys. Two types each of marcasite, pyrite, and wurtzite, and one type of sphalerite are observed in all three active chimneys.

3) The extinct chimney lacks the outer anhydrite-rich and Fe–Zn-rich zones, probably because of dissolution by cold seawater. The exterior wall is a chalcopyrite-rich layer; the conduit is clogged by pyrite, marcasite, wurtzite and sphalerite which have different crystal habits compared to those in the active chimneys.

4) Similarities in the temporal and spatial relationships among different types of Fe and Zn sulfides, anhydrite, and chalcopyrite in the active chimneys, and the relationships between the size of conduit opening and the thicknesses and composition of various mineralogical zones in both the active and extinct chimneys suggest that the processes of chimney growth were similar at all vent sites of 11° and 13°N, and that each chimney represents a different stage of maturity and preservation of a complete (ideal) chimney.

5) A complete chimney consists of 8 mineralogical zones (or facies). From outside to inside of the chimney, they are: 1 (anhydrite with minor marcasite + pyrite + wurtzite), 2 (marcasite + wurtzite + minor anhydrite), 3 (pyrite + sphalerite), 4 (nearly monomineralic bornite), 5 (nearly monomineralic chalcopyrite), 6 (pyrite + sphalerite), 7 (marcasite + wurtzite), and 8 (wurtzite + pyrite). Zones 1 to 5 develop during the outward growth (waxing stage) of chimneys, whereas zones 6 to 8 develop during the filling (waning stage) of chimney conduits.

6) The growth of chimneys is initiated by the formation of the facies-1 assemblage, which takes place as a result of rapid mixing of hydrothermal fluids and cold seawater. The outward growth of chimneys occurs by: (i) successive transformation of facies-1 minerals into facies-2, -3, -5, and -4 minerals by reactions with Fe-, Zn-, Cu- and H_2S-bearing fluids in the interior of the chimneys; and (ii) formation of new layers of facies-1 minerals at the exterior of the chimneys. Therefore, all mineralogical zones (1–5) inherit, to a varying degree, the fluid characteristics (T and metal compositions) of the entire stage (rather than a particular stage) of hydrothermal activity; minerals in the outer zones inherit higher proportions of the earlier fluid characteristics. The chimney-growth processes are analogous to skarn formation, with a major difference in the material that is replaced by sulfide minerals (anhydrite *versus* limestone).

7) Previous researchers (Eldridge *et al.* 1983) have suggested that anhydrite-rich layers play an important role in the development of sulfide chimneys and volcanogenic massive sulfide deposits by acting as a thermal blanket for sulfide ore. Our model suggests that anhydrite may also play an important chemical role for the development of FeS_2-rich sulfide ores by providing various oxidation mechanisms to produce polysulfide species from hydrothermal H_2S.

8) Kinetics of various oxidation reactions seem to control the mineralogy of Fe sulfides (pyrrhotite, marcasite and pyrite) in a chimney. The kinetics of nucleation are also important in the formation of wurtzite *versus* sphalerite.

9) Monomineralic zones of chalcopyrite and pyrite develop because of the preferential replacement of ZnS over FeS_2 by chalcopyrite during the chimney growth stage. Replacement of chalcopyrite by FeS_2 may occur during the waning stage of hydrothermal activity.

10) Chimneys of higher maturity are characterized by larger conduit openings, better developed monomineralic zones of pyrite, chalcopyrite and bornite, and higher ratios of Σsulfide/anhydrite, Cu/Fe and Fe/Zn. Differences between the Zn-rich *versus* Cu-rich chimneys may be a function of the maturity of a chimney, rather than of fluid temperature.

REFERENCES

BALLARD, R.C., HÉKINIAN, R. & FRANCHETEAU, J. (1984): Geological setting of hydrothermal activity at 12°50'N on the East Pacific Rise: a submersible study. *Earth Planet. Sci. Lett.* **69**, 176-186.

BARTON, P.B., JR. (1973): Solid solutions in the system Cu–Fe–S. Part 1. The Cu–S and Cu–Fe–S join. *Econ. Geol.* **68**, 455-465.

_____ (1978): Some ore textures involving sphalerite from the Furutobe mine, Akita Prefecture, Japan. *Mining Geol.* **28**, 293-300.

_____ & TOULMIN, P., III (1964): The electrum-tarnish method for the determination of the fugacity of sulfur in laboratory sulfide systems. *Geochim. Cosmochim. Acta* **28**, 619-640.

_____ & _____ (1966): Phase relations involving sphalerite in the Fe–Zn–S system. *Econ. Geol.* **61**, 815-849.

BLUTH, G. & OHMOTO, H. (1988): Sulfide–sulfate chimneys on the East Pacific Rise, 11° and 13°N latitudes. Part II: sulfur isotopes. *Can. Mineral.* **26**, 505-515.

BOWERS, T.S., VON DAMM, K.L. & EDMOND, J.M. (1985): Chemical evolution of mid-ocean ridge hot springs. *Geochim. Cosmochim. Acta* **49**, 2239-2252.

_____, CAMPBELL, A.C., MEASURES, C.I., SPIVACK, A.J., KHADEM, M. & EDMOND, J.M. (1988): Chemical controls on the composition of vent fluids at 13°–11°N and 21°N, East Pacific Rise. *J. Geophys. Res.* **93**, 4522-4536.

CABRI, L.J. (1973): New data on phase relations in the Cu–Fe–S system. *Econ. Geol.* **68**, 443-454.

_____, HALL, S.R., SZYMAŃSKI, J.T. & STEWART, J.M. (1973): On the transformation of cubanite. *Can. Mineral.* **12**, 33-38.

CAMPBELL, A.C., BOWERS, T.S., MEASURES, C.I., FALKNER, K.K., KHADEM, M. & EDMOND, J.M. (1988): A time series of vent fluid compositions from 21°N, East Pacific Rise (1979, 1981, 1985), and the Guaymas Basin, Gulf of California (1982, 1985). *J. Geophys. Res.* **93**, 4537-4549.

CRAIG, J.R. & VAUGHAN, D.J. (1981): *Ore Microscopy and Ore Petrography.* John Wiley & Sons, New York.

CRERAR, D.A. & BARNES, H.L. (1976): Ore solution chemistry V. Solubilities of chalcopyrite and chalcocite assemblages in hydrothermal solutions at 200°C to 350°C. *Econ. Geol.* **71**, 772-794.

DREVER, J.I. (1982): *The Geochemistry of Natural Waters.* Prentice-Hall, Englewood Cliff, N.J.

DUTRIZAC, J.E. (1976): Reactions in cubanite and chalcopyrite. *Can. Mineral.* **14**, 172-181.

ELDRIDGE, C.S., BARTON, P.B., JR. & OHMOTO, H. (1983): Mineral textures and their bearing on formation of the Kuroko orebodies. *Econ. Geol. Monogr.* **5**, 241-281.

EDMOND, J.M., MEASURES, C., MANGUM, B., GRANT, B., SCLATER, F.R., COLLIER, R., HUDSON, A., GORDON, L.I. & CORLISS, J.B. (1979): On the formation of metal-rich deposits at ridge crests. *Earth Planet. Sci. Lett.* **46**, 19-30.

GOLDFARB, M.S., CONVERSE, D.R., HOLLAND, H.D. & EDMOND, J.M. (1983): The genesis of hot spring deposits in the East Pacific Rise, 21°N. *Econ. Geol. Monogr.* **5**, 184-197.

GOLDHABER, M.B. & STANTON, M.R. (1987): Experimental formation of marcasite at 150–200°C; implications for carbonate hosted Pb/Zn deposits. *Geol. Soc. Amer. Program Abstr.* **19**.

HAYMON, R.M. (1983): Growth history of hydrothermal black smoker chimneys. *Nature* **301**, 695-698.

_____ & KASTNER, M. (1981): Hot spring deposits on the East Pacific Rise at 21°N: preliminary description of mineralogy and genesis. *Earth Planet. Sci. Lett.* **53**, 363-381.

HÉKINIAN, R., FEVRIER, M., BISCHOFF, J.L., PICOT, P. & SHANKS, W.C. (1980): Sulfide deposits from the East Pacific Rise near 21°N. *Science* **207**, 1433-1444.

_____, FRANCHETEAU, J., RENARD, V., BALLARD, R.D., CHOUKROUNE, P., CHEMINÉE, J.L., ALBAREDE, F., MINSTER, J.F., CHARLOU, J.L., MARTY, J.C. & BOULEGUE, J. (1983): Intense hydrothermal activity at the axis of the East Pacific Rise near 13°N: submersible witnesses the growth of a sulfide chimney. *Marine Geophys. Res.* **6**, 1-14.

_____ & FOUQUET, Y. (1985): Volcanism and metallogenesis of axial and offaxial structures on the East Pacific Rise near 13°N. *Econ. Geol.* **80**, 221-249.

KOSKI, R.A., CLAGUE, D.A. & OUDIN, E. (1983): Mineralogy and chemistry of massive sulfide deposits from the Juan de Fuca Ridge. *Geol. Soc. Amer. Bull.* **95**, 930-945.

KUSAKABE, M., CHIBA, H. & OHMOTO, H. (1982): Stable isotopes and fluid inclusion study of anhydrite from the East Pacific Rise at 21°N. *Geochem. J.* **16**, 89-95.

McCONACHY, T.F., BALLARD, R.C., MOTTL, M.J. & VON HERZEN, R.P. (1986): Geological form and setting of a hydrothermal vent field at lat 10°56'N, East Pacific Rise: a detailed study using Angus and Alvin. *Geology* **14**, 295-298.

MUROWCHICK, J.B. & BARNES, H.L. (1984): The recognition and significance of porous pyrite. *Geol. Soc. Amer. Program Abstr.* **16**, 604.

_____ & _____ (1986a): Formation of cubic FeS. *Amer. Mineral.* **71**, 1243-1246.

_____ & _____ (1986b): Marcasite precipitation from hydrothermal solutions. *Geochim. Cosmochim. Acta* **50**, 2615-2629.

NORMARK, W.R., MORTON, J.L., BISCHOFF, J.L., BRETT, R., HOLCOMB, R.T., KAPPEL, E.S., KOSKI, R.A., ROSS, S.L., SHANKS, W.C., SLACK, J.F., VON DAMM, K.L. & ZIERENBERG, R.A. (U.S.G.S. Juan de Fuca Study Group) (1986): Submarine fissure eruptions and hydrothermal vents along the southern Juan de Fuca Ridge: Preliminary observations from the submersible ALVIN. *Geology* **14**, 823-827.

OHMOTO, H. (1988): Formational processes of volcanogenic massive sulfide deposits. *In* Hydrothermal Processes – Applications to Ore Genesis (H.L. Barnes & H. Ohmoto, eds.). D. Reidel Publishing Co., Dordrecht, Holland (in press).

_____, MIZUKAMI, M., DRUMMOND, S.E., ELDRIDGE, C.S., PISUTHA-ARNOND, V. & LENAGH, T.C. (1983): Chemical processes of Kuroko formation. *Econ. Geol. Monogr.* **5**, 570-567.

_____ & SKINNER, B.J. (1983): The Kuroko and related volcanogenic massive sulfide deposits: Introduction and summary of new findings. *Econ. Geol. Monogr.* **5**, 1-8.

OUDIN, E. (1983): Hydrothermal sulfide deposits of the East Pacific Rise (21°N). Part 1: descriptive mineralogy. *Mar. Mining* **4**, 39-72.

SPIESS, F.N., MACDONALD, K.C., ATWATER, T., BALLARD, R., CARANZA, A., CORDOBA, D., COX, C., DIAZ GARCIA, V.M., FRANCHETEAU, J., GUERRERO, J., HAWKINS, J., HAYMON, R., HESSLER, R., JUTEAU, T., KASTNER, M., LARSON, R., LUYENDYK, B., MACDOUGALL, J.D., MILLER, S., NORMARK, W., ORCUTT, J. & RANGIN, C. (1980): East Pacific Rise: hot springs and geophysical experiments. *Science* **207**, 1421-1433.

STYRT, M.M., BRACKMANN, A.J., HOLLAND, H.D., CLARK, B.C., PISUTHA-ARNOND, V., ELDRIDGE, C.S. & OHMOTO, H. (1981): The minerology and the isotopic composition of sulfur in hydrothermal sulfide/sulfate deposits on the East Pacific Rise, 21°N latitude. *Earth Planet. Sci. Lett.* **53**, 382-390.

TIVEY, M.D. & DELANEY, J.R. (1986): Growth of large sulfide structures on the Endeavour Segment of the Juan de Fuca Ridge. *Earth Planet. Sci. Lett.* **77**, 303-317.

TUNNICLIFFE, V., BOTROS, M., DE BURGH, M.E., DINET, A., JOHNSON, H.P., JUNIPER, S.K. & McDUFF, R.E. (1986): Hydrothermal vents of Explorer Ridge, northeast Pacific. *Deep-Sea Res.* **33**, 401-412.

TURNER, J.S. & CAMPBELL, I.H. (1987): A laboratory and theoretical study of the growth of "black smoker" chimneys. *Earth Planet. Sci. Lett.* **82**, 36-48.

VON DAMM, K.L. (1988): Systematics of and postulated controls on submarine hydrothermal solution chemistry. *J. Geophys. Res.* **93**, 4551-4561.

_____ GRANT, B. & EDMOND, J.M. (1983): Preliminary report on the chemistry of hydrothermal solutions at 21°N, East Pacific Rise. *In* Hydrothermal Processes at Seafloor Spreading Centers (P.A. Rona, K. Böstrom, L. Laubier & K.L. Smith, Jr., eds.). Plenum Press, New York, 369-390.

WELHAN, J.A. & CRAIG, H. (1983): Methane, hydrogen and helium in hydrothermal fluids at 21°N on the East Pacific Rise. *In* Hydrothermal Processes at Seafloor Spreading Centers (P.A. Rona, K. Böstrom, L. Laubier & K.L. Smith, Jr., eds.). Plenum Press, New York, 391-410.